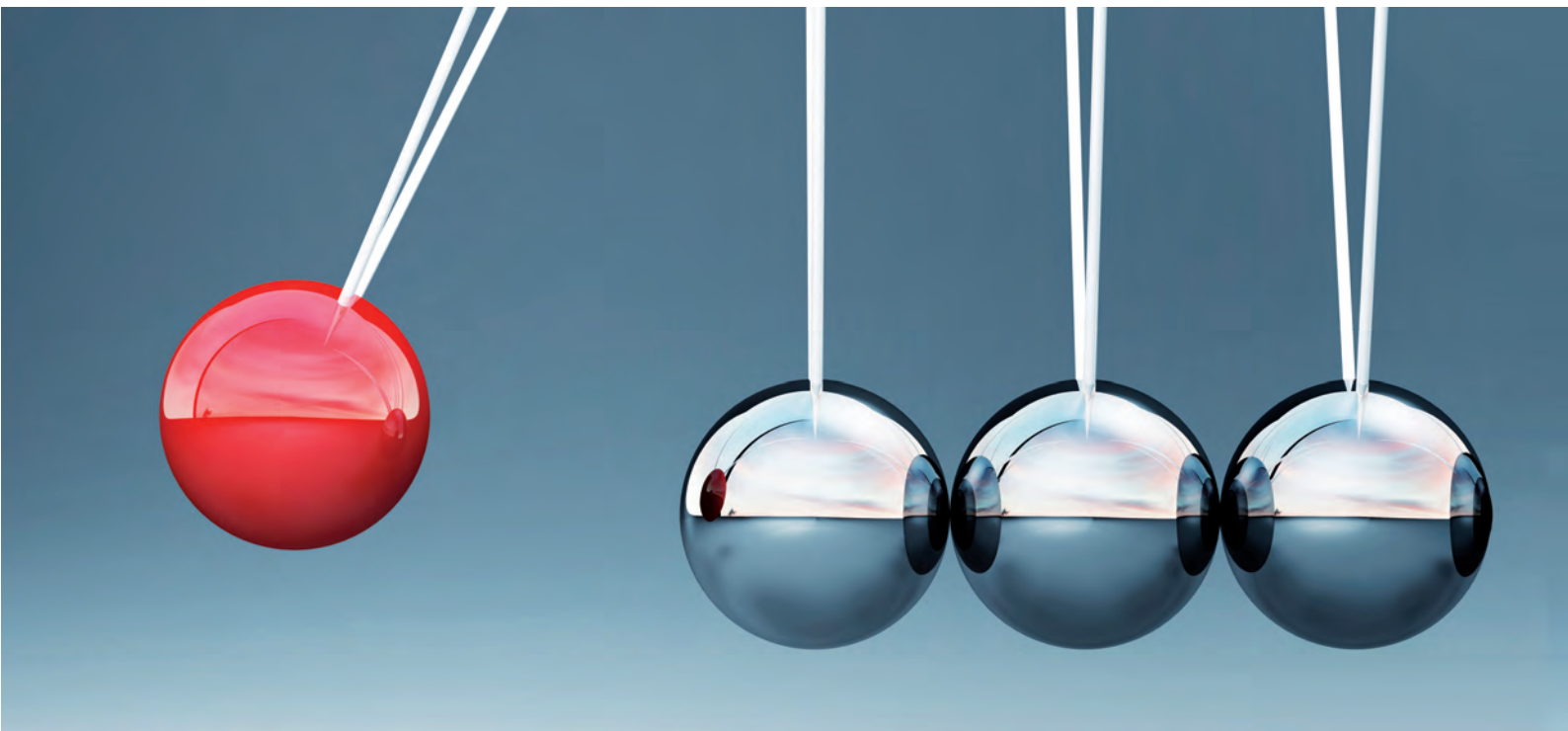P5856

HeNe Laser Frequency Stabilisation   4747111 EN

LEYBOLD®

Laser Sicherheitshinweise

Hiermit erklärt die Firma LD Didactic GmbH,

dass es sich bei dem angebotenen Lasersystem um einen Aufbau handelt, der sowohl in Komponenten als auch im fertigen Aufbau einem Laser der Klasse 3A, 3B oder 4 nach DIN EN 60 825-1 entspricht. Typischerweise ist die Pumpdiode eine Nd:YAG Laser Klasse 4, ein HeNe Laser mit Auskoppler Klasse 3A, aber ein HeNe mit zwei hochreflektierenden Spiegeln nur Klasse 1. Bitte die Anleitung oder Aufkleber beachten.

Aus Haftungsgründen dürfen diese Geräte oder Gerätesammlungen nicht an Privatleute verkauft werden. Der Einsatz von Lasern oberhalb Klasse 2 an allgemeinbildendenden Schulen ist in Deutschland nicht gestattet.

Gewerbliche Abnehmer, Schulen und Universitäten werden hiermit darauf hingewiesen, dass aus dem missbräuchlichen Betrieb der Geräte ein Verletzungsrisiko, speziell für die Augen, resultiert.

Dem Benutzer obliegt insbesondere:
- Die relevanten Unfallverhütungsvorschriften zu beachten, zur Zeit beispielsweise BGV B2 und BGI 832
- die OstrV zu beachten „Verordnung zum Schutz der Beschäftigten vor Gefährdungen durch künstliche optische Strahlung"
- Der Betrieb der Geräte muss rechtzeitig beim Gewerbeaufsichtsamt und der Berufsgenossenschaft angezeigt werden.
- Der Betreiber muss schriftlich einen Laserschutzbeauftragten benennen, der für die Einhaltung der Schutzmaßnahmen verantwortlich ist.
- Die Geräte sind nur für den Betreib in umschlossenen Räumen vorgesehen, deren Wände die Ausbreitung des Laserstrahls begrenzen.
- Der Laserbereich ist deutlich und dauerhaft zu kennzeichnen.
- Ab Laserklasse 4 ist eine Laser-Warnleuchte am Raumzugang notwendig.

- Die Geräte sind zur Lehre und Ausbildung in Berufsschulen, Universitäten oder ähnlichen Einrichtungen gedacht.
- Die Geräte nur innerhalb der in den Anleitungen vorgegebenen Betriebsbedingungen betreiben.
- Die Geräte nur von entsprechend unterwiesenen Mitarbeitern und Studierenden benutzen lassen. Bei Handhabung des Gerätes durch Studenten müssen diese von entsprechend geschultem Personal überwacht werden.

Als praktische Ratschläge:

- Vor dem Einschalten auf Beschädigungen prüfen

- Nicht in den Strahl blicken

- Den Laserstrahl so führen, dass sich keine Personen, Kinder oder Tiere ungewollt im Strahlbereich befinden können

- Den Laserstrahl nicht auf reflektierende Flächen oder in den freien Raum richten

- Nicht mit reflektierenden Gegenständen im Laserstrahl arbeiten

- Armbanduhr, Schmuck und andere reflektierende Gegenstände ablegen.

- Beim Einsetzen optischer Bauteile den Laserstrahl an der Quelle abschalten oder geeignet abdecken, bis die Bauteile positioniert sind

- Teilweise wird mit unsichtbaren Laserstrahlen gearbeitet, deren Verlauf nicht sichtbar ist.

- Falls nötig, Laserschutzbrillen oder Laserjustierbrillen benutzen.

Die Firma LD Didactic GmbH haftet nicht für eine missbräuchliche Verwendung der Geräte durch den Kunden.

Der Kunde verpflichtet sich hiermit die Geräte nur entsprechend der rechtlichen Grenzen einzusetzen und insbesondere den Laserstrahl nicht im Straßenverkehr oder Luftraum zu verwenden oder in anderer Form auf Personen und Tiere zu richten.

Der Kunde bestätigt, das er befugt ist, diesen Laser zu erwerben und zu verwenden.

Laser Safety Notes

LD Didactic GmbH informs the customer this is laser equipment of either class 3A, 3B or 4 according to IEC 60 825. Typically a Nd:YAG Pump Diode is class 4, a HeNe with output coupler class 3A, but a HeNe with two high reflecting is mirrors only class 1. Please see manual or attached labels for the exact specification of the laser.

Special safety precautions are necessary. Please check with local regulations. Typically the use requires a safety sign and a warning lamp that is on when the laser is activated and it might also be necessary to do and document a risk assessment.

Due to product liability, the laser must not be sold to individual persons. Companies, higher schools and universities might use it, but are notified that misuse of the laser poses a health risk, especially for the eyes.

The intended use of this equipment is for lessons, education and research in higher schools, universities or similar institutions.

Do not operate the devices outside parameters specified in the manual.

People using the laser must be properly trained and students must be supervised.

As a general guidance, the user is advised to:

- Check the laser for damages before use

- Not to look into the beam

- Take necessary measures that no people or animals can accidentally enter the beam area

- do not direct the beam on reflecting surfaces or into public areas

- do not work close to the light path with reflecting tools

- take off all jewelry and wristwatches when working with the laser to avoid reflections

- While placing or removing optical parts in the light path, switch off the laser or cover its exit

- Some of the experiments use invisible laser beams, but still might hurt the eye

- use laser protection glasses or laser adjustment glasses where necessary

- supervise students by trained personnel when they work with the laser system

- use the laser system only as described in the instruction manuals

Customer acknowledges the receipt of this information.

The customer indemnifies LD Didactic from liability for any damages that occur because of misuse of the laser.

The customer confirms that he will obey all local regulations and is allowed by law to buy and use the laser system.

Table of Contents

1.0 Introduction

The Helium-Neon laser was the first continuous laser. It was invented by Javan et. al. in 1961. Nowadays lasers are usually pre-adjusted using a He-Ne laser. The similarity between the manufacturing techniques of He-Ne lasers and electron valves helped in the mass production and distribution of He-Ne lasers. The replacement of tubes by transistors in the sixties left a sufficiently redundant production capacity. In Germany for example, the Siemens tube factory took over this production and has produced over one million He-Ne lasers to date.

It is now clear that He-Ne lasers will have to increasingly compete with laser diodes in the future. But He-Ne lasers are still unequalled as far as beam geometry, the purity of the modes and frequency stability are concerned.

Laser diodes will have to be improved to a great extent before they pose a serious threat to He-Ne lasers in this regard. The major application of HeNe laser are found in laser metrology like laser gyroscopes for navigation and laser interferometer for the precise calibration of CNC machines. Due to the achievable high degree of frequency stability HeNe laser can be used as secondary standards for the length. The basic principle of distance measurement is based on the counting of the bright to dark transitions created by an interferometer. The measured distance Lx is calculated as

$$L_x = N \cdot \frac{\lambda}{2}$$

whereby N is the number of counted fringes (dark-bright transitions) and λ the wavelength of the used light source. It is obvious that the precision of the measurement depends on the wavelength λ and the accuracy of determining N. The free running HeNe laser already provides an accuracy of the wavelength of

$$\frac{\delta\lambda}{\lambda} = 1 \cdot 10^{-6}$$
.

In practise it means an accuracy of 1μm on 1 metre. For the calibration of industrial CNC machines however an accuracy of 10^{-8} and above is required. Within this experiment we introduce the frequency stabilisation of such a HeNe laser by using the so called two mode stabilisation scheme. The term "frequency" stabilisation is used, if we are completely in vacuum we also could have termed "wavelength stabilisation".

In addition we will demonstrate the Zeeman splitting by using a permanent magnet converting the HeNe laser into a "Zeeman laser". The gained results are discussed as an other possibility for frequency stabilisation.

2.0 Fundamentals

2.1 He-Ne energy- level diagram

The fascination for inert gases and their clear atomic structure formed the basis for many spectroscopic investigations. The knowledge obtained through spectroscopic data was extremely helpful in deciding to choose helium and neon for the first lasers, using Schawlow Towne's discovery of lasing conditions in 1958 to estimate whether an inversion was feasible in laser operation. The lifetime of

the s- and p-states were well known. Those of the s-states were longer than those of the p-states by a factor of about 10. The inversion condition was therefore fulfilled.
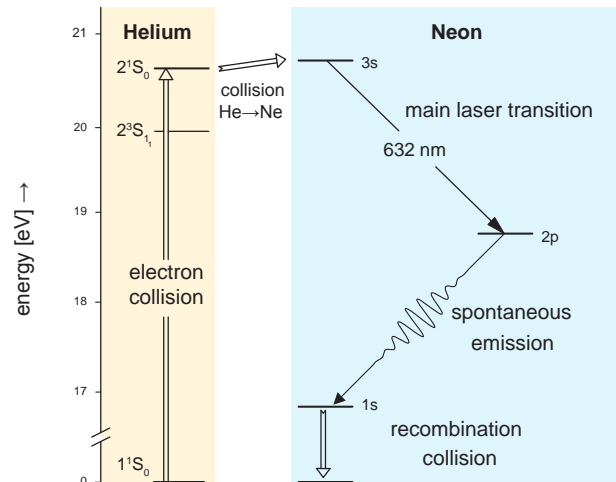

Fig. 1: Excitation and Laser process for the visible Laser emission

Fig. 1 shows the reduced energy-level diagram for helium and neon. Only those levels important in the discussion of the excitation and laser processes at a wavelength of 632 nm are indicated.

The left side of the representation shows the lower levels of the helium atoms. Observe how the energy scale is interrupted and that there is a larger difference in energy in the recombination process than is evident in the diagram. Paschen's names for the neon energy levels are used (Racah's term descriptions are often found as well). The terms are simply numbered consecutively, from bottom to top. A characteristic of helium is that its first states to be excited, 2^1S_1 and 2^1S_0 are metastable, i.e. optical transitions to the ground state 1^1S_0 are not allowed, because this would violate the selection rules for optical transitions. As a result of gas discharge, these states are populated by electron collisions (collision of the second type, Fig. 2).

A collision is called a collision of the second type if one of the colliding bodies transfers energy to the other so that a transition from the previous energy state to the next higher or lower takes place. Apart from the electron collision of the second type there is also the atomic collision of the second type. In the latter, an excited helium atom reaches the initial state because its energy has been used in the excitation of a Ne atom. Both these processes form the basis for the production of a population inversion in the Ne system.
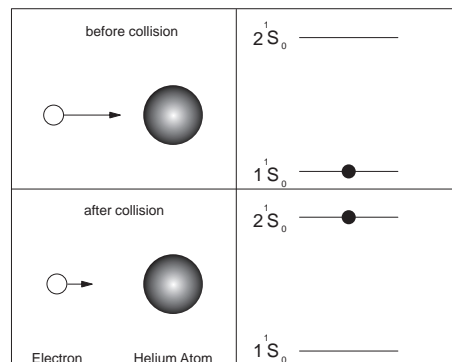

Fig. 2: Electron collision of the second kind

If we look at Fig. 1 we can see that the 2^1S_0 is slightly below the 3s level of the neon. However, the additional thermal energy kT is sufficient to overcome this gap.

As already mentioned, the lifetime of the s-states of the neon are approximately 10 times longer as those of the p-states. An immediate population inversion between the 3s and the 2p levels will therefore be generated. The 2s level is emptied due to spontaneous emission into the 1s level. After this the neon atoms reaching their ground state again, primarily through collisions with the tube wall (capillary), since an optical transition is not allowed. This calming down process is the bottle neck in the laser cycle. It is therefore advisable to choose a capillary diameter that is as small as possible. However, the laser will then suffer more losses. Modern He-Ne lasers work at an optimum of these contradictory conditions. This is the main reason for the comparatively low output of He-Ne lasers.

We have discussed the laser cycle of the commonly known red line at 632 nm up to this point. However the neon has several other transitions, used to produce about 200 laser lines in the laboratories. The following explanation describes the energy-level diagram for further visible lines. After that infrared laser transitions will be discussed.
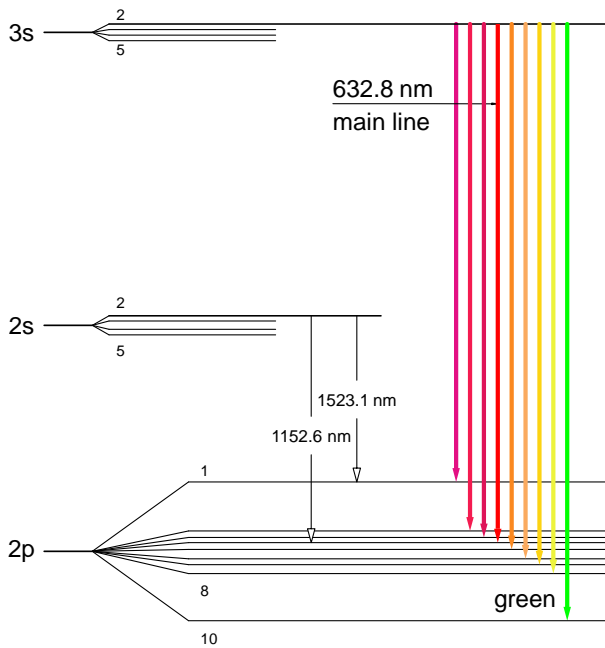
Fig. 3: The most important laser transitions in the neon system

The 3s state is populated by Helium atoms of the 2^1S_0, state as a result of an atomic collision. The 3s state consists of 4 sub-states out of which it is primarily the $3s_2$ state which has been populated through the collision process. The population density of the other 3s sub-states is app. 400 times less than that of the $3s_2$ state. The 2s state is populated by the Helium atoms of the 2^3S_1, as a result of an atomic collision.

The four sub-states of the 2s group are all populated in a similar way. Visible (VIS) optical transitions and laser processes are taking place between the 3s2 → 2pi and infrared (IR) between the 2si → 2pi energy levels.

The Table 1 shows the most important laser transitions. The Einstein coefficients A_{ik} are given for the visible lines and amplification is indicated as a percentage per meter.

Further laser transitions are known, which start at the 3s2 level and terminating at the 3p level of the neon. However, these laser transitions lie even further within the infrared spectral range and cannot be detected with the silicon detector used in the experiment. They are not particularly suitable for experiments. Notice that these lines are originating from the same level as the visible lines and are therefore competing with them.

Since the cross-section of the stimulated emission is increasing with λ^3 as well, the amplification of these lines is therefore very strong. This applies to the 3.39 μm line in particular, which, due to a sufficiently long capillary, shows laser activity (so called super fluorescence) even without an optical resonator.

Transition	Wavelength [nm]	A_{ik} [10^8 s^{-1}]	Gain [%/m]	
$3s_2 \rightarrow 2p_1$	730.5	0,00255	1,2	①
$3s_2 \rightarrow 2p_2$	640.1	0,0139	4,3	①
$3s_2 \rightarrow 2p_3$	635.2	0,00345	1,0	①
$3s_2 \rightarrow 2p_4$	632.8	0,0339	10,0	①
$3s_2 \rightarrow 2p_5$	629.4	0,00639	1,9	①
$3s_2 \rightarrow 2p_6$	611.8	0,00226	1,7	①
$3s_2 \rightarrow 2p_7$	604.6	0,00200	0,6	
$3s_2 \rightarrow 2p_8$	593.9	0,00255	0,5	
$3s_2 \rightarrow 2p_9$	Transition not allowed			
$3s_2 \rightarrow 2p_{10}$	543.3	0,00283	0,52	
$2s_2 \rightarrow 2p_1$	1523.1			③
$2s_2 \rightarrow 2p_2$	1177.0			②
$2s_2 \rightarrow 2p_3$	1160.5			
$2s_2 \rightarrow 2p_4$	1152.6			②
$2s_2 \rightarrow 2p_5$	1141.2			②
$2s_2 \rightarrow 2p_6$	1084.7			②
$2s_2 \rightarrow 2p_7$	1062.3			
$2s_2 \rightarrow 2p_8$	1029.8			
$2s_2 \rightarrow 2p_9$	Transition not allowed			
$2s_2 \rightarrow 2p_{10}$	886.5			
$2s_3 \rightarrow 2p_2$	1198.8			②
$2s_3 \rightarrow 2p_5$	1161.7			②
$2s_3 \rightarrow 2p_7$	1080.1			②

Table 1: Transitions and Laser lines

①   Laser transition is demonstrated provided set of mirrors
②   Laser transitions are demonstrated in the experiment with optional IR mirror set
③   Laser transitions are demonstrated with special mirror set

Appropriate measures must be taken to suppress the super fluorescence to avoid a negative influence on the visible laser lines.
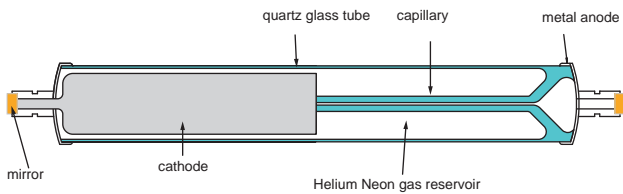
Fig. 4: **Modern He-Ne laser with glass-to-metal soldering of the anode, cathode and laser mirror**

Fig. 4 shows a modern laser tube made with highly perfected manufacturing techniques and optimised to suit the physical aspects of the laser. This applies to the resonator in particular, which is designed for a best possible output in the fundamental mode with a purely Gaussian beam and spectral purity in single mode operation (e.g. for interferometric length measurement). The fulfilment of this demand depends, amongst other aspects, on the optimal adaptation of the resonator to the amplification profile of the Neon. The behaviour of Neon during amplification will therefore be discussed first.

2.2 Amplification

The Neon atoms move more or less freely in the laser tube but at different speeds. The number N of neon atoms with the mass m, within a speed interval of v to v+dv is described according to the Maxwell-Boltzmann distribution Fig. 5.

$$\frac{n(v)}{N} = \frac{4}{\sqrt{\pi}} \cdot \frac{v^2}{\sqrt[3]{(2kT/m)^2}} \cdot e^{-\frac{mv^2}{k \cdot T}} dv$$

T is the absolute temperature and k Boltzmann´s constant The above equation is applicable for all directions in space. However, we are only interested in the distribution of speed in the direction of the capillary. Using $v^2 = v_x^2 + v_y^2 + v_z^2$ we obtain for the direction x:

$$\frac{n(v_x)}{N} = \sqrt{2kT/m} \cdot e^{-\frac{m \cdot v^2}{k \cdot T}} dv_x \qquad \textbf{Eq. 2.1}$$

A resting observer will now see the absorption or emission frequency shifted, due to Doppler's effect (Ch. Doppler: Abh. d. K. Boehmischen Ges. d. Wiss. (5). Vol. II (1842) P.465), and the value of the shift will be:

$$\nu = \frac{\nu_0}{1 \pm v/c} \qquad \text{assuming } v \ll c \qquad \textbf{Eq. 2.2}$$

ν_0 is the absorption or emission frequency of the resting neon atom and c the speed of light. If the Doppler equation (Eq. 2.1)is used to substitute the velocity v in the Maxwell-Boltzmann´s velocity distribution (Eq. 2.2) the line broadening produced by the movement of Neon atoms can be found. Since the intensity is proportional to the number of absorbing or emitting Neon atoms, the intensity distribution will be:

$$I(v) = I(v_0) \cdot e^{-\left(c \cdot \frac{V - V_0}{V_0 \cdot V_w}\right)^2} \qquad \textbf{Eq. 2.3}$$

v_w is the most likely speed according to:

$$v_w = \sqrt{\frac{2kT}{m}}$$
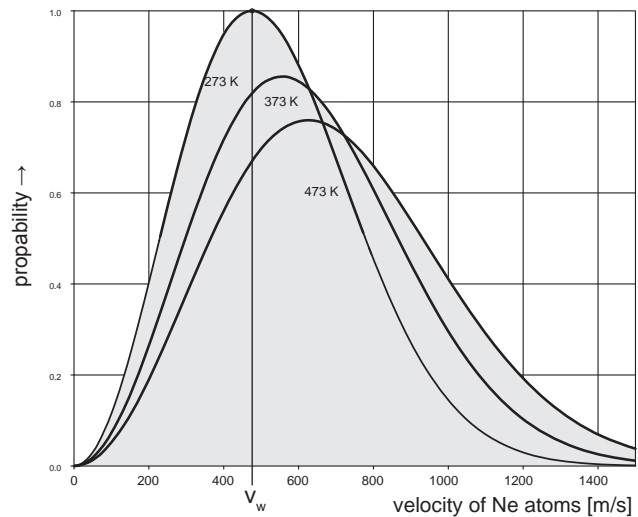
Fig. 5: **Probability Distribution for the velocity v of the neon atoms within the interval v to v + dv.**

The full width at half maximum is calculated by setting I(n)=1/2 I(n_0) and the result is:

$$\Delta v_{Doppler} = \sqrt{4 \cdot \ln 2} \cdot \frac{v_w}{c} \cdot v_0 \qquad \textbf{Eq. 2.4}$$

We can conclude from Eq. 2.4 that the line broadening caused by Doppler's effect is larger in the case of:

> higher resonance frequencies ν_0
> or smaller wavelengths ($\nu_0 = c/\lambda_0$, UV - lines)
> higher most likely velocity v_w
> that means higher temperature T

and smaller in the case of:

> a larger particle mass.

The line profile also corresponds to a Gaussian distribution curve (Eq. 2.3). Fig. 6 shows this kind of profile. The histogram only approaches the distribution curve when the speed intervals dv are small.
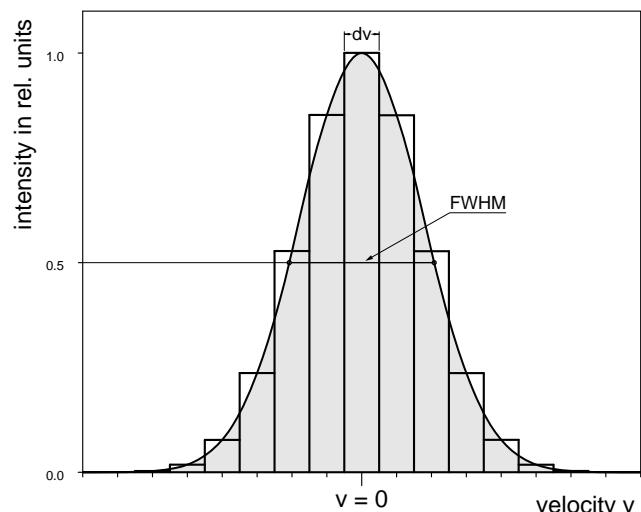
Fig. 6: **Inhomogeneous line profile, speed intervals dv**

Why these speed intervals dv or frequency intervals dν you may ask. Actually there are formal reasons for this. Not having any intervals at all would be like wanting to make a statement on fishing out a particle with an exact speed or frequency from the ensemble. It is almost impossible to do. So, we define finite probabilities of ensembles by using intervals. If we succeed in this, we can make the intervals smaller and work with "smooth curves".

On closer observation we can see that a line broadened by the Doppler effect actually does not have a pure Gaussian distribution curve.

To understand this, we pick out an ensemble of Ne atoms whose speed components have the value v in the direction we are looking at. We expect that all these atoms emit light with the same frequency ν or wavelength λ. But we have to consider an additional effect which is responsible for the natural line width of a transition. We know that each energy level poses a so called life time. The population n_2 of a state 2 decays into a state 1 with lower energy with a time constant τ_s following the equation :

$$n_2(t) = n_2(t=0) \cdot e^{-A_{21} \cdot t} \qquad \tau_s = \frac{1}{A_{21}}$$

A_{21} is the famous Einstein coefficient for the spontaneous emission. The emission which takes place is termed as spontaneous emission.
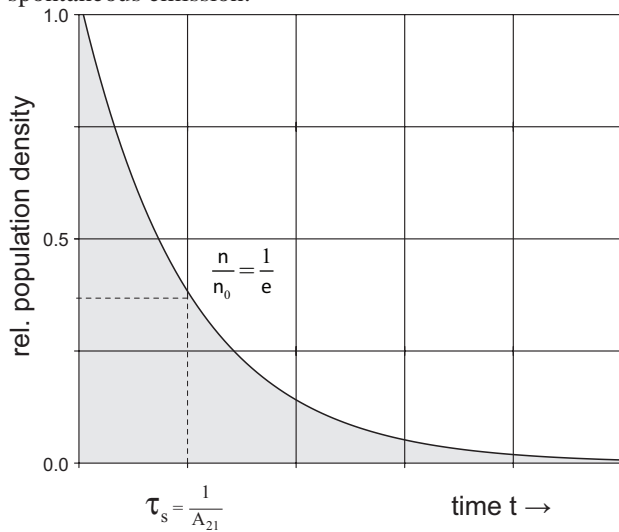

Fig. 7: Decay of the population of state 2 into a state 1 with lower energy

This shows us, that the ensemble of Ne atoms does not emit light at a single frequency. It emits a frequency spectra represented by an Lorentz profile (Fig. 8).

$$\delta(v) = \frac{1}{4\pi \cdot (v - v_{21})^2 + (1/2 \cdot \tau_s)^2}, v_0 \equiv v_{21}$$
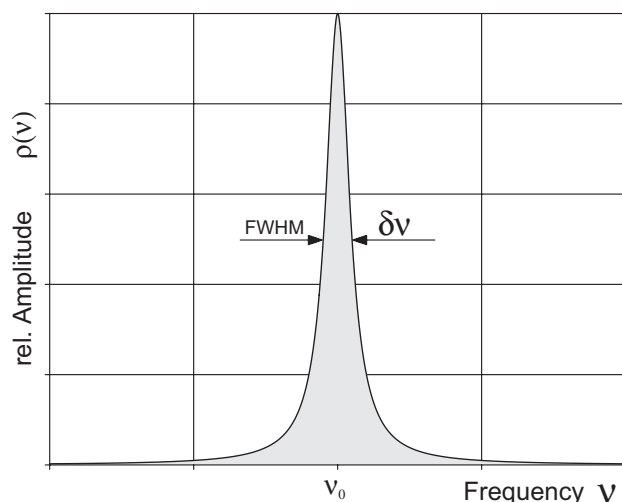

Fig. 8: Natural linewidth (FWHM) caused by spontaneous emission

The exact profile formation can be determined from the convolution of the Gaussian profile with the individual Lorentz profiles. The result obtained in this manner is called as the Voigt profile. Since one group of particles in an ensemble can be assigned to a given speed v, these groups have characteristics that differentiate them. Every group has its own frequency of resonance. Which group a photon interacts with depends on the energy (frequency) of the photon. This does not affect the other groups which are not resonant on this interaction. Therefore such kind of a gain profile is termed inhomogeneous.
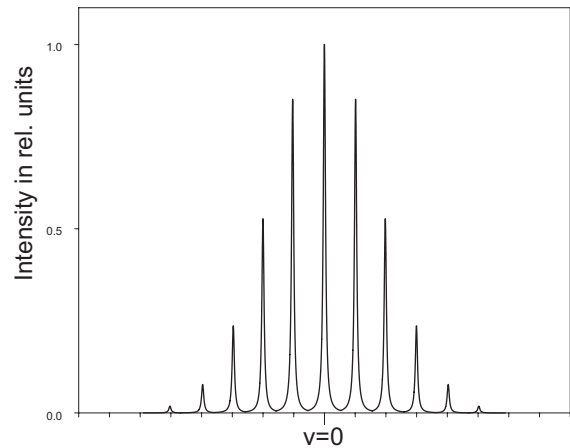

Fig. 9: Natural broadened line profiles (homogeneous) for groups of speed v within the inhomogeneous Doppler broadened gain profile

As we already know gain occurs in a medium when it shows inversion. This means that the population density of the upper level n_2 (3s in the Ne-system) is larger than the population density of the lower state n_1 (2p). In Fig. 10 the population profiles are rotated by 90° to draw them in the well known energy level diagram. Transition can only take place between sub-ensembles which have the same velocity v because the optical transition does not change the speed of the particular Ne atom.
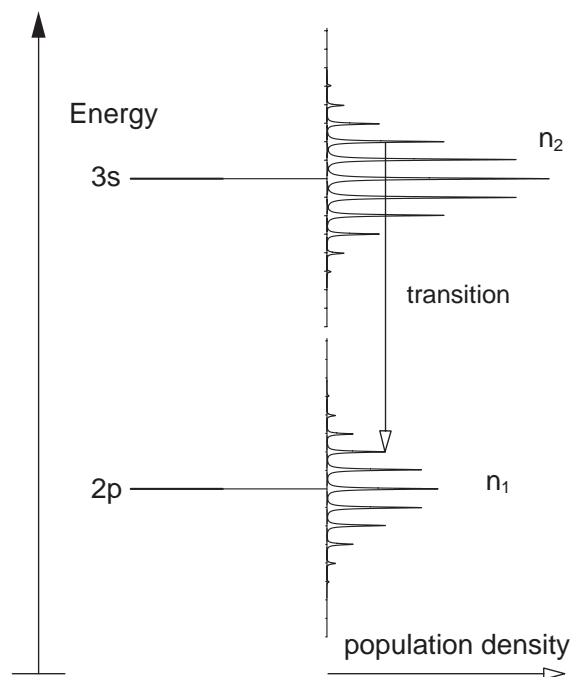

Fig. 10: Population inversion and transition between sub-ensembles with same velocity v

Page 7

The situation of Fig. 10 shows a population inversion $n_2 > n_1$. Besides some specific other constants the gain is proportional to the difference $n_2 - n_1$. Now we will place the inverted ensemble of Ne atoms into an optical cavity, which is formed by two mirrors having the distance of L. Due to the spontaneous emission photons are generated which will be amplified by the inverted medium and reflected back from the mirrors undergoing a large number of passes through the amplifying medium.
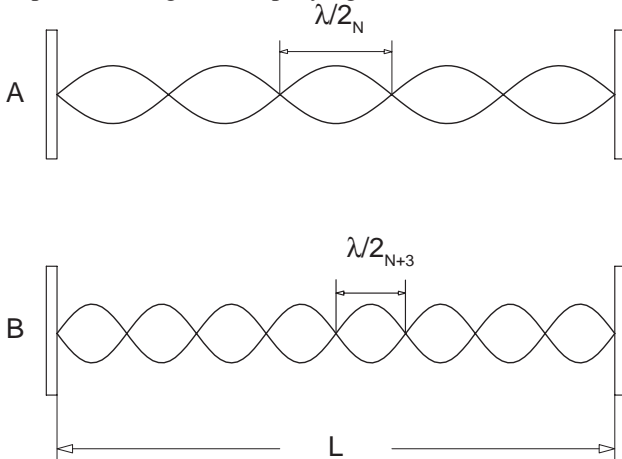
Fig. 11: Standing longitudinal waves in an optical resonator. A with N nodes and B with N+3 nodes

If the gain compensates for the losses, a standing laser wave will be built up inside the optical resonator. Such a standing wave is also termed as oscillating mode of the resonator also eigenmode or simply mode. Every mode must fulfil the following condition:

$$L = N \cdot \frac{\lambda}{2} \text{ or } L = N \cdot \frac{c}{2\nu} \qquad \textbf{Eq. 2.5}$$

L represents the length of the resonator, λ the wavelength, c the speed of light, ν the frequency of the generated light and N is an integer number. Thus every mode has its frequency of

$$\nu(N) = N \cdot \frac{c}{2L}$$

e.g. A He-Ne-Laser with a resonator length of 30 cm at an emission wavelength λ of 632.8 nm will have the following value for n:

$$N = \frac{\nu}{c} \cdot 2 \cdot L = 2 \cdot \frac{L}{\lambda} = 2 \cdot \frac{0,3}{632,8 \cdot 10^{-8}} = 949.167$$

The difference in frequency of two neighboured modes is:

$$\Delta\nu = \nu(N+1) - \nu(N)$$
$$= (N+1) \cdot \frac{c}{2L} - N \cdot \frac{c}{2L} = \frac{c}{2L} \qquad \textbf{Eq. 2.6}$$

In the above example the spectral distance between modes would be

$$\Delta\nu = \frac{3 \cdot 10^8}{2 \cdot 0,3} = 5 \cdot 10^8 \, \text{Hz} = 500 \, \text{MHz}$$

If the active laser material is now brought into the resonator standing waves will be formed due to the continuous emission of the active material in the resonator and energy will be extracted from the material. However, the resonator can only extract energy for which it is resonant. Strictly speaking, a resonator has an indefinite amount of modes, whereas the active material only emits in an area of frequency determined by the emission line width.

Fig. 12 shows the situation in the case of material that is inhomogeneously broadened.
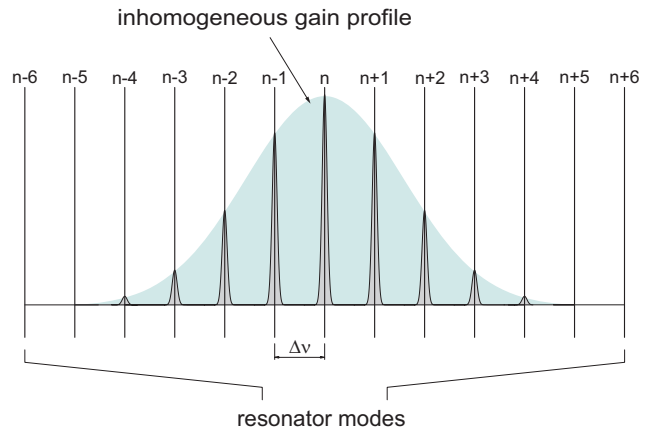
Fig. 12: Inhomogeneously broadened gain profile (Gaussian profile) interacting with an optical resonator

If the laser is operating in a stationary state, we can see that it is emitting several longitudinal modes. These are exactly the same modes that will be found in the emission profile. Since the modes are fed by an inhomogeneous emission profile they can also exist independently. The He-Ne-Laser is a classic example of this.

2.3 Laser mode sweeping

Within the frame of the upcoming practical work we will use a laser tube which emits only two modes. This can be achieved by choosing the cavity length L in such a way that the spectral distance is about 800 MHz. This results in a cavity length of 19 cm.
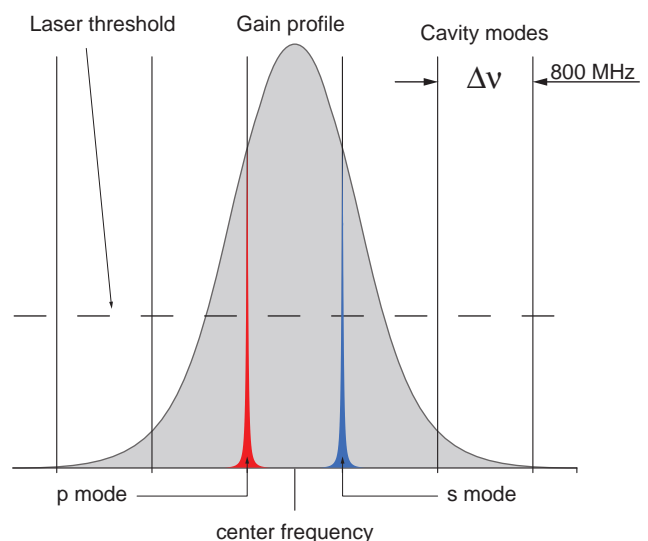
Fig. 13: Longitudinal Cavity Modes

In reality the length L is generally not constant and varies due to thermal expansion leading to the so called mode

sweeping. The effect of thermal expansion or changing the length by δL we calculate from the already introduced resonance condition Eq. 2.5

$$\nu = N \cdot \frac{c}{2 \cdot L}$$

we obtain:

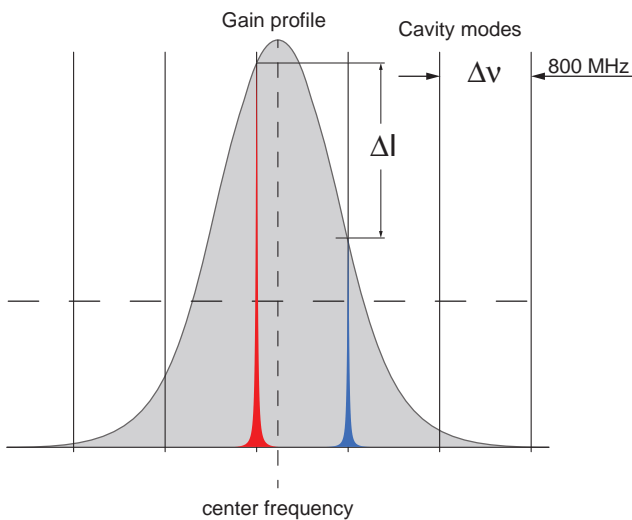$$\partial \nu = -N \cdot \frac{c}{2L} \partial L$$

by using:

$$L = N \cdot \frac{\lambda}{2}; \; N = \frac{2L}{\lambda}$$

we finally get:

$$\partial \nu = -\frac{2L}{\lambda} \cdot \frac{c}{2L} \partial L = \frac{c}{\lambda} \cdot \partial L$$

$$\partial \nu = -\frac{3 \cdot 10^8}{632.8 \cdot 10^{-9}} \cdot \partial L = -4.75 \cdot 10^{14} \cdot \partial L$$

The thermal expansion of quartz glass, from which the cavity of a HeNe laser tube is made is $5.1 \cdot 10^{-7}$ per degree Kelvin. That means a change of 1°K would cause a change of already 242 MHz!

**Fig. 14: Mode sweep of 242 MHz due to 1° K temperature change**

Fig. 14 shows the mode sweep of 242 MHz caused by a temperature change of 1°K. It can be seen that the intensity of one mode drops and the other increases(ΔI). In Fig. 13 both modes have the same intensity and are centred symmetrically to the well known resonance frequency. To keep the two modes in this condition we need to have a controller which senses the intensity of both modes and controls the length of the cavity. This leads to the idea of a two mode stabilisation scheme.

Before we close this chapter and discussing the stabilisation scheme we need to understand one further aspect of laser modes, the mode competition. From the spectroscopic data of Table 1 we know that the laser transition starts from the $^3s_2$ level and ends at $^2p_4$. The "fuel" of the laser transition comes from the population inversion created in the $^3s_2$ level. In the case here two modes are in need for "fuel" and it is a brutal rule that the winner takes it all.

Despite this fact two or even more modes can exist unless they are fed from different sources. One of this "classification" of sources is due to the Doppler effect as described in chapter 2.2. Another aspect is given due to the fact of polarisation. Statistically seen the created photons due to the transition $^3s_2 \rightarrow {}^2p_4$ are 50% polarised lets say horizontal and 50% orthogonal to it. We know from quantum mechanics that orthogonal states do not interact and can be considered as independent from each other. This the modes know and therefore one takes the opposite polarisation of the other one resulting in the emission of two orthogonal linear polarised modes. By means of a polarising beam splitter both modes can be separated and there intensity measured independently from each other.

2.4 Two Mode Stabilisation
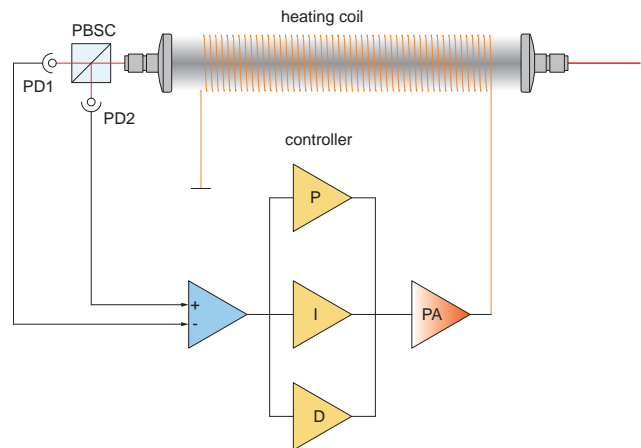
Fig. 15: Schematic of two mode stabilisation scheme

From Fig. 14 we learned that the equal intensity of both modes exist only when they are centred symmetrical to the gain profile. A PID controller receives the difference of both modes and by means of a heating coil wound around the laser tube is used to control the length L of the cavity in such a way that the intensity difference of both modes is theoretically zero or practically constant.
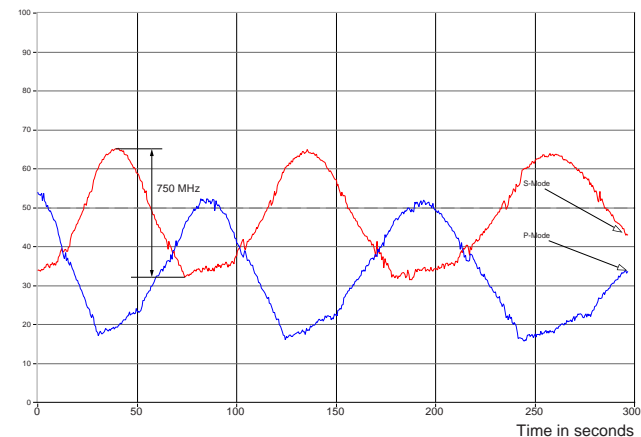

Fig. 16: Mode sweep taken right after switching on the laser taken with the provided software

The Fig. 16 shows the intensity of each mode versus the time. After switching on the laser, it takes about 30 minutes to reach thermal stability. The sweeping of the modes can clearly be seen. From the maximum to the minimum peak the mode "travelled" approximately the half of the gain profile (depending on the laser threshold) of 750

MHZ. This gives a good scale for the frequency drift.
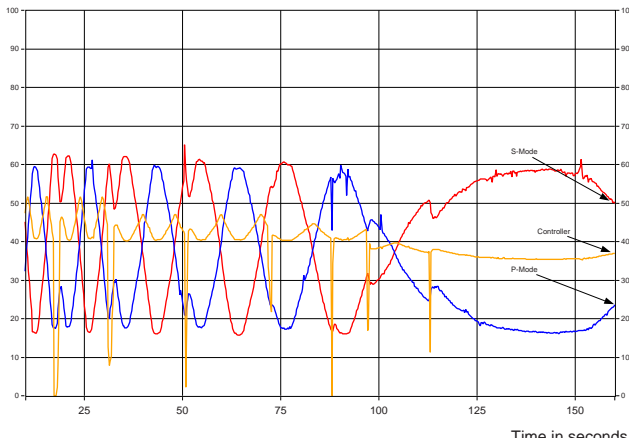
**Fig. 17: Plot of the control software while adjusting the control parameter**

After activating the PID controller the proportional parameter P, the integral I and derivative D parameter needs to be adjusted to lock the controller to best frequency stability. At this point we will not explain the basics of control circuits, however it is essential to understand the concept. The action of the controller can be described as:

$$S(t) = K_p \cdot e(t) + K_i \int_0^t e(\tau) d\tau + K_d \frac{d}{dt} e(t)$$

Depending on the time constant and frequence response of the controlled system the parameter K_p, K_i and K_d needs to be adjusted accordingly. The function $e(t)$ is the timely varying deviation, in our case the intensity difference of both modes. The gaols of the controller is to make $e(t)$ zero. There are two possible best practices to achieve this. One is the analytical one. Based on some system parameter initial values for K_p, K_i and K_d are obtained. The other one is try and error or better said "educated guessing". For this purpose the control software provides a chart strip to set the parameter while observing the mode behaviour

3.0 Zeeman Effect

We will not again derive the Zeeman effect here just recall the important facts.
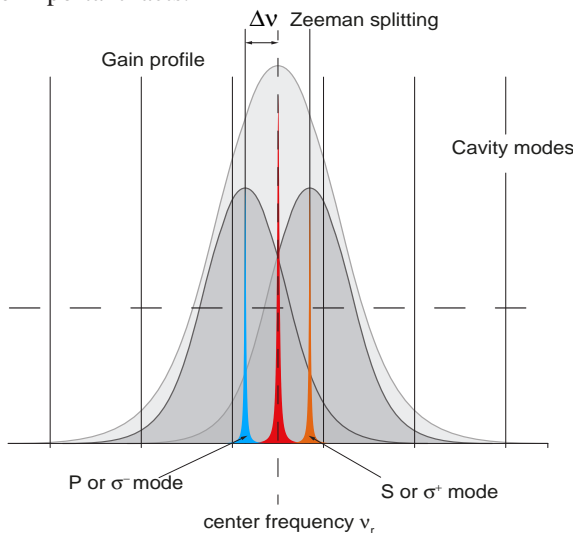
**Fig. 18: Zeeman splitting of the gain profile with relevant**

laser modes

We consider the HeNe laser operating at the dominant transition $^3s_2 \rightarrow {}^2p_4$ at a wavelength of 632 nm (see also Table 1). Applying a magnetic field either longitudinal or transversal to the cavity axis will split the involved energy levels of the Neon. As a result we obtain for each allowed transition a gain profile as shown in Fig. 18. Because the applied magnetic field does not cover all Neon atoms some transitions remain which are not split. Even if the magnetic field covers only a fraction of the laser tube these transition will dominantly remain. Under such conditions we should expect beside the appearance of the main line two additional modes having a frequency of $v_r \pm \Delta v$ caused by the Zeeman splitting.

However, the reality is different since we also have to take the laser dynamics into consideration. In this regards we need to introduce the frequency pulling and pushing effects as well as the mode competition. To understand the frequency pulling and pushing we need to understand the anomalous dispersion. The normal dispersion we commonly know from glass prisms or from birefringent materials.

$$n_{o,e}^2(\lambda) = A_{o,e} + \frac{B_{o,e} \cdot \lambda^2}{\lambda^2 - C_{o,e}} + \frac{D_{o,e} \cdot \lambda^2}{\lambda^2 - F_{o,e}}$$

The standard equation for normal dispersion is valid only for those values of the wavelength which are not close to a resonant transition. A, B, C, D and F are material constants.
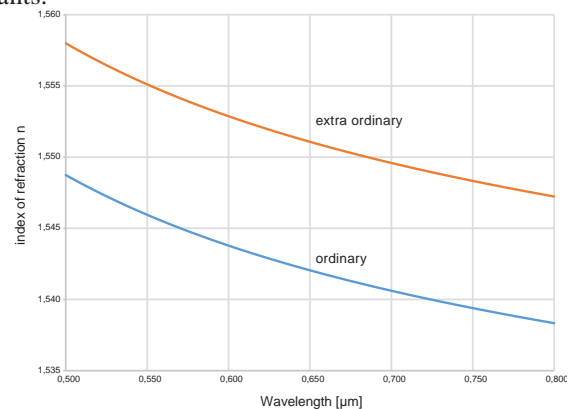
Fig. 19: Normal dispersion of quartz

The anomalous dispersion occurs close to the centre frequency of a transition. The Fig. 20 shows the variation of the index of refraction close to the resonance of a transition.
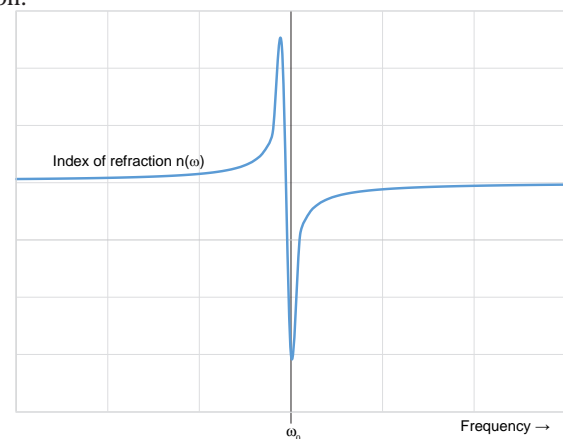
Fig. 20: Index of refraction close to the centre frequency of a transition

From the previous chapter we know that an empty cavity is resonant when the condition

$$L = N \cdot \frac{\lambda}{2}$$

is fulfilled. L stands for the mechanical length of the cavity. N is an integer and λ for the wavelength. If we are placing a material with index of refraction n into the cavity then the resonance condition modifies to:

$$n \cdot L = N \cdot \frac{\lambda}{2}$$

Instead of the mechanical length L it is now required that the optical length $n \cdot L$ is a multiple of half of the wavelength. We are not just putting some material into the cavity, no, it will be a laser active one. Such active material provides transitions like $^3s_2 \rightarrow {}^2p_4$ in the case of Ne. Of course we need to rewrite the resonance condition to

$$n(\omega) \cdot L = N \cdot \frac{\pi \cdot c}{\omega_0} \qquad \textbf{Eq. 2.7}$$

This is an important consideration. The laser itself controls its frequency by pulling or pushing the laser mode in such a way that a suitable $n(\omega)$ will be obtained to fulfil the above condition (Eq. 2.7).

If for instance the mechanical length L is changing due to thermal or other effects the laser will tune its frequency resulting in a suitable $n(\omega)$. This is why a laser for metrology purposes needs a stabilisation to provide a known and constant wavelength or frequency.

Coming back to the Zeeman effect, our resonance condition needs to be fulfilled also for the split frequencies ω^- and ω^+:
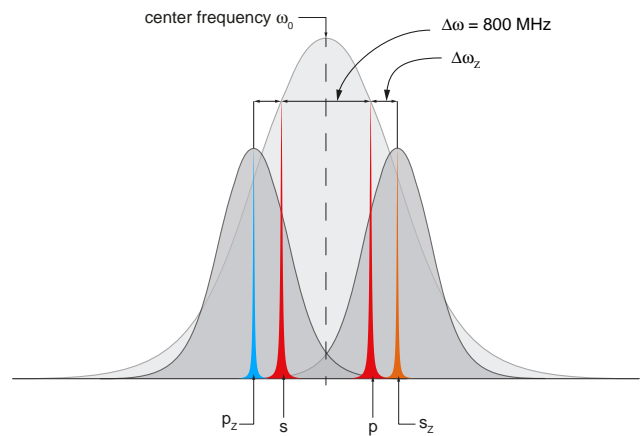
$$n(\omega \pm \Delta\omega) \cdot L = N \cdot \frac{\pi \cdot c}{(\omega_0 \pm \Delta\omega)}$$

Finally we have to have a look to mode competition effects.
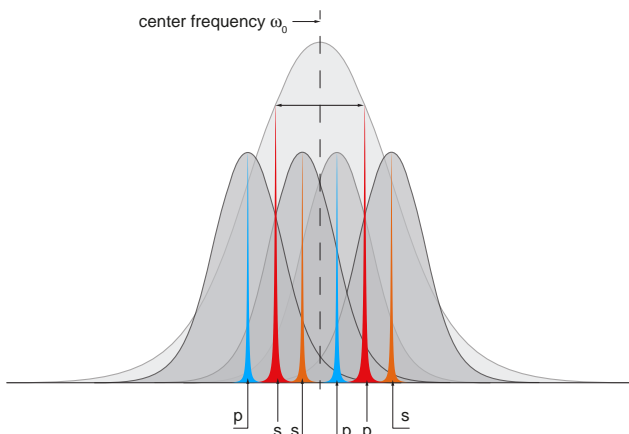
Fig. 21: Complete set of possible Zeeman modes

In the Fig. 21 the possible extra modes due to the Zeeman splitting are shown. However the close neighboured modes with same polarisation s or p will collapse to one mode in favour of the strongest one as shown in Fig. 22.

**Fig. 22: Residual modes due to mode competition effects.**

In fact the Laser emits now 4 modes with a combination of beat frequencies of
A.   800 MHz + 2·$\Delta\omega_z$
B.   800 MHz + $\Delta\omega_z$
C. $\Delta\omega_z$
Where by $\Delta\omega_z$ is the caused by Zeeman splitting as well frequency pulling and pushing effects of the laser.
The shunt of the photodetector is switched to such a value (10 kΩ) that beyond 100 MHz no signals will be detected. Therefore we just detect the beat frequency caused by the Zeeman splitting and the dynamic of the HeNe laser. During the experiment it will be noticed that the beat frequency is not constant and only present if the laser cavity is tuned close to the centre frequency.

4.0 Description of the components
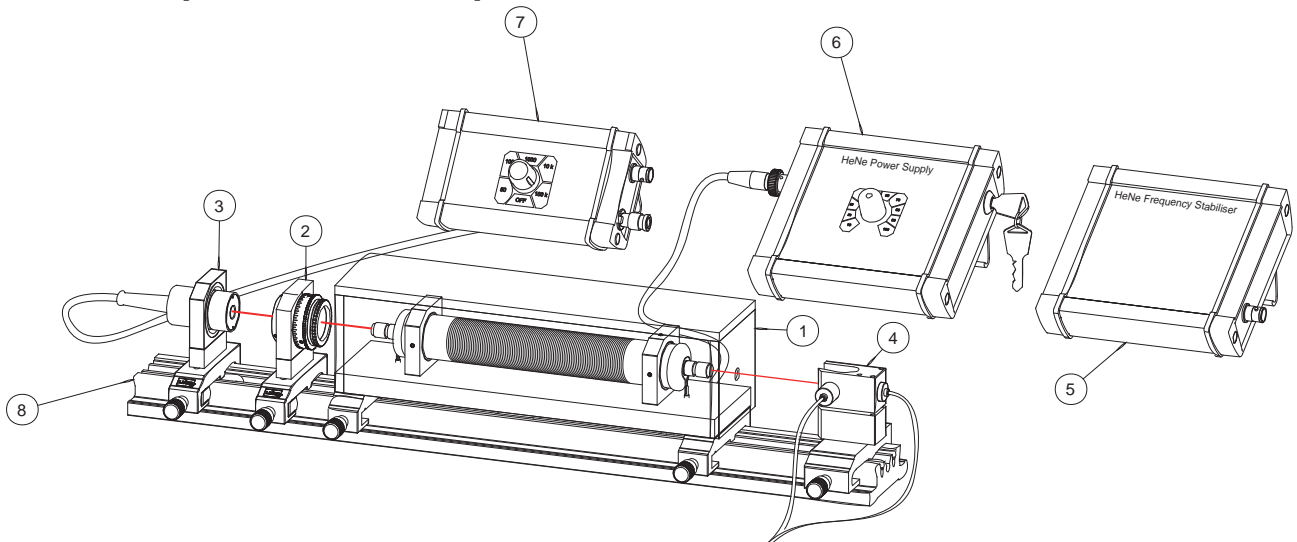
Fig. 23: Setup of the experiment for the frequency stabilisation of a HeNe Laser
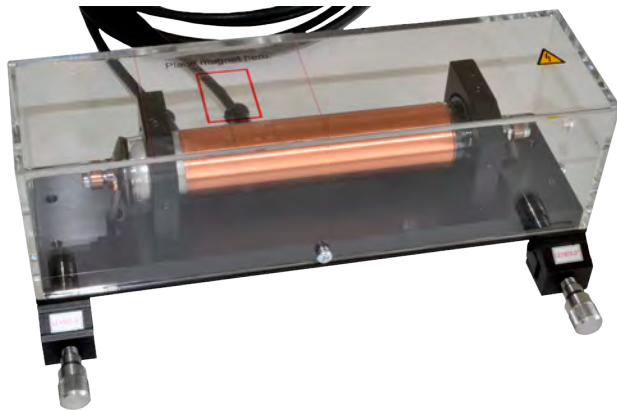
Fig. 24: Helium Neon laser tube (1)

A Helium Neon laser tube (1) is covered by a acrylic housing for security reasons. A small fraction of the main laser intensity leaves the tube which is used for the stabilisation. The tube is supplied with the necessary high voltage of the high voltage supply(6). The length of the laser tube is chosen in such a way that a two mode emission results. In this case both modes are orthogonally polarised to each other. A part of the laser tube is covered by a bifilar heater coil. By means of the frequency stabiliser device (5) the two coils can be switched of to observe the Zeeman effect of a free running HeNe laser.

Fig. 25: Zeeman magnet

The magnet is a strong NdFeB Magnet and consists of 7 pieces with a dimension of (L x B x H) 4 x 20 x 10 mm. The material is classified as N 35 and the remanence of a single element is 1.21 T. Do not separate the magnets, they are brittle and might crush when recombining. Other safety rules of dealing with magnets must be applied. By placing the magnet on top of the cover of the laser tube inside the red marked area (Fig. 25) causes the Zeeman

splitting and as observed as beat frequency detected with the photodiode (3).

Fig. 26: High voltage power supply (6)

The high voltage tube controller supplies the Helium Neon laser tube with the needed high voltage for ignition and operation. The key switch located at the side panel prevents unauthorized switching on of the laser. A switched wall plug power supply is provided which is connected via the right panel side. The laser tube is connected via a high voltage BNC connection to the controller. The discharge current can be set by the switch located on the front panel from 4.5 to 6.75 mA in steps of 0.25 mA. Within this experiment the current shall be set to 5.5 mA.

Fig. 27: Frequency stabilizer electronics (5)

The HeNe frequency stabiliser contains a full digital operating PID controller. Via the USB bus the provided software the controller parameter of the proportional, integral and derivative properties are set. The signal of the two photodiodes of the mode separator (4) are forming the input of a differential amplifier. Amplification and offset of the stage can be set by the software. This signal is the input of the actual value of the controller. Based on the set target value the controller provides an output signal which is amplified and used to heat more or less the laser tube. By means of the central switch the heater coil can be switched off to observe the Zeeman effect.
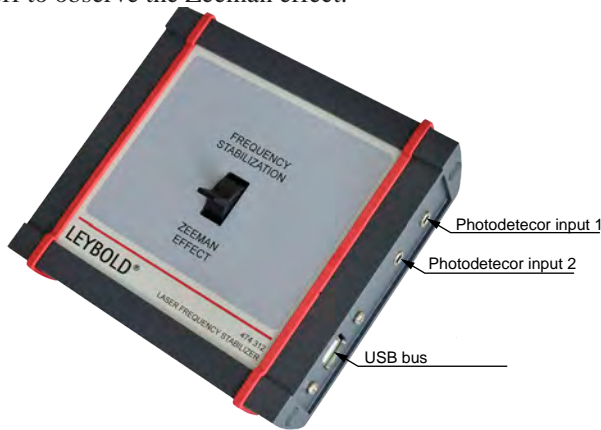
Fig. 28: In and output connector of the frequency stabiliser

Fig. 29: Adjustable polariser (2)

In a rotational ring mount with a 360°, scale a polariser is assembled. In case the incident light is polarized, a minimum intensity occurs indicating that the polariser is adjusted 90° with respect to the polarisation direction of the incident light. The rotator has a scale gradation from 0 - 360° at intervals of 5°. The unit is made out of special anodized aluminium and can be directly attached to the optical rail (8) by means of the attached carrier 20 mm. A high quality acrylic sheet polariser is contained in a C25 optics mount.

Fig. 30: Mode separation module (4)

To separate two orthogonal modes in order to determine

the intensity of each one, a polarising beam splitter cube is used. Behind the cube, two photodetector (Fig. 31) are attached under an angle of 90° to each other to measure the intensity of each mode. The mode separator is attached to a carrier for the optical rail (8).

Fig. 31: Mini Photodetector for the mode separation module

The Si PIN photodetector is accommodated inside a small housing with as diameter of 12 mm. The photodiode is connected to a screened connection lead with a 3.5 mm stereo jack which fits into the input of the PID controller unit (5).

Fig. 32: Photodetector connecting device (7)

This device allows the connection of the photodetector to an oscilloscope or muiltimeter. For this purpose the photoelectric current which is proportional to the number of incident photons needs to be converted into a voltage. The device is driven by a 9 V battery which lasts almost one year under regular operation. The impedance of the output can be adjusted from 50 Ohms to 100 k. The "OFF" position still provides via an 1 M Ohm shunt a signal with a very high sensitivity which sometimes is useful. For fast signals the lower shunt resistors are used. Rise times of 2 ns can be measured in the 50 and 100 position.

Fig. 33: SiPIN photodetector (3)

The photodiode is mounted into a housing which can be inserted in 25 mm mounting plates. The signal is available at the connected cable with 6 pin PS/2 connector to be connected to the photodetector connecting device(7).

5.0 Software

The software requires Microsoft Windows (XP to WIN8) operating system. Furthermore DOTNET 4 and the driver for the USB serial (FTDI) needs to be installed. The operation software as well as mentioned drivers are located on the provided DVD.

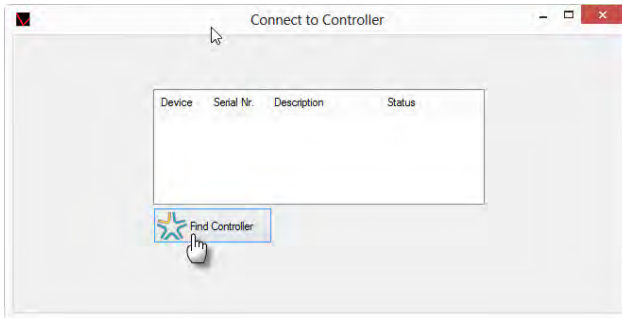After starting the software the following device connecting sequence needs to be passed.

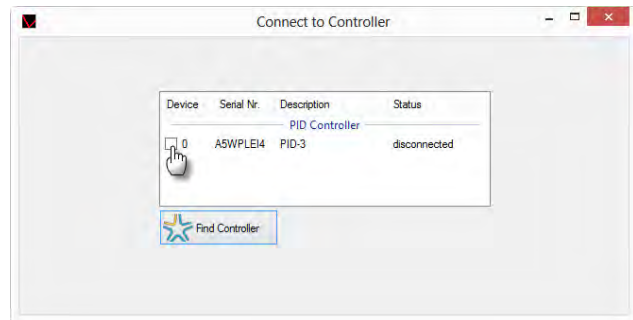**Fig. 34: Click to find controller on the system**
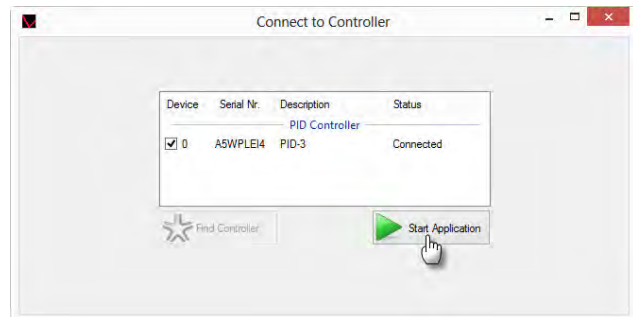

Fig. 35: Select the controller PID-03

Fig. 36: Start the controller application
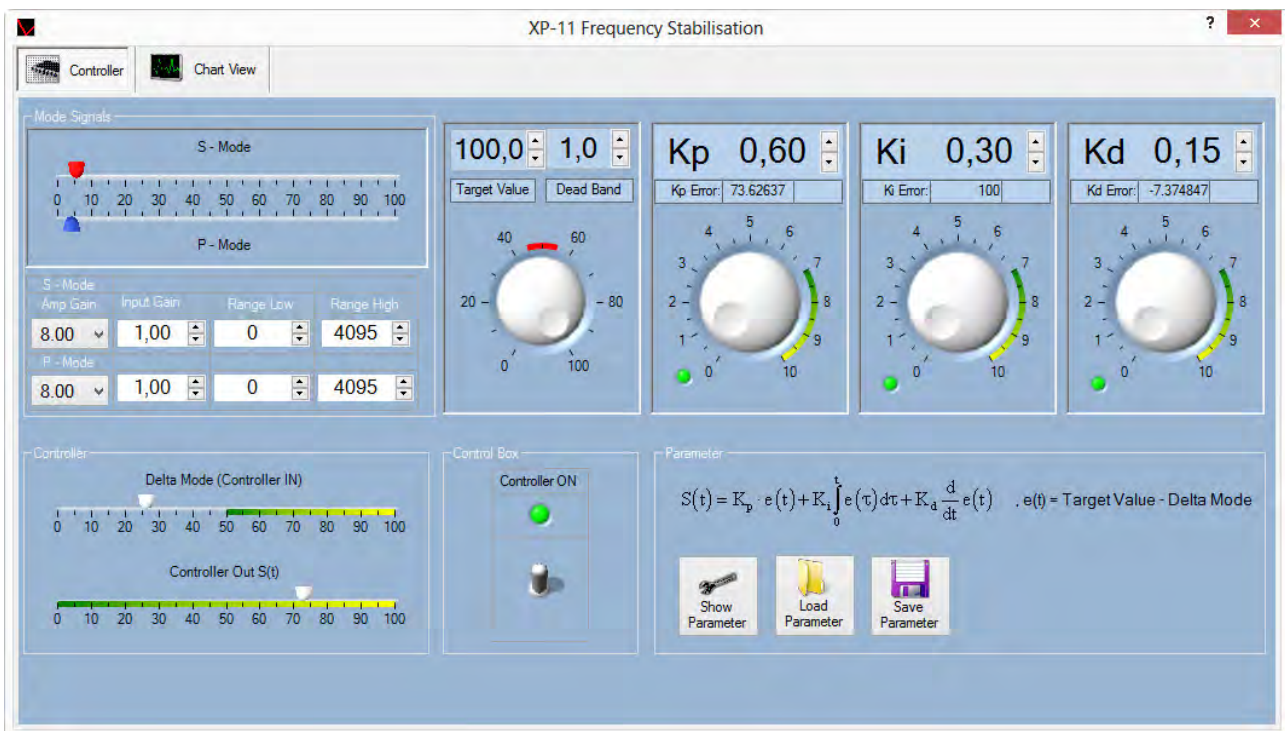
Fig. 37: Main screen of the controller software

In the control box of the window a question mark is located. Clicking on it and selecting a control brings up the individual help information and instructions. By means of the buttons "Show, Load and Save" parameter the entire set of controller settings can be managed.
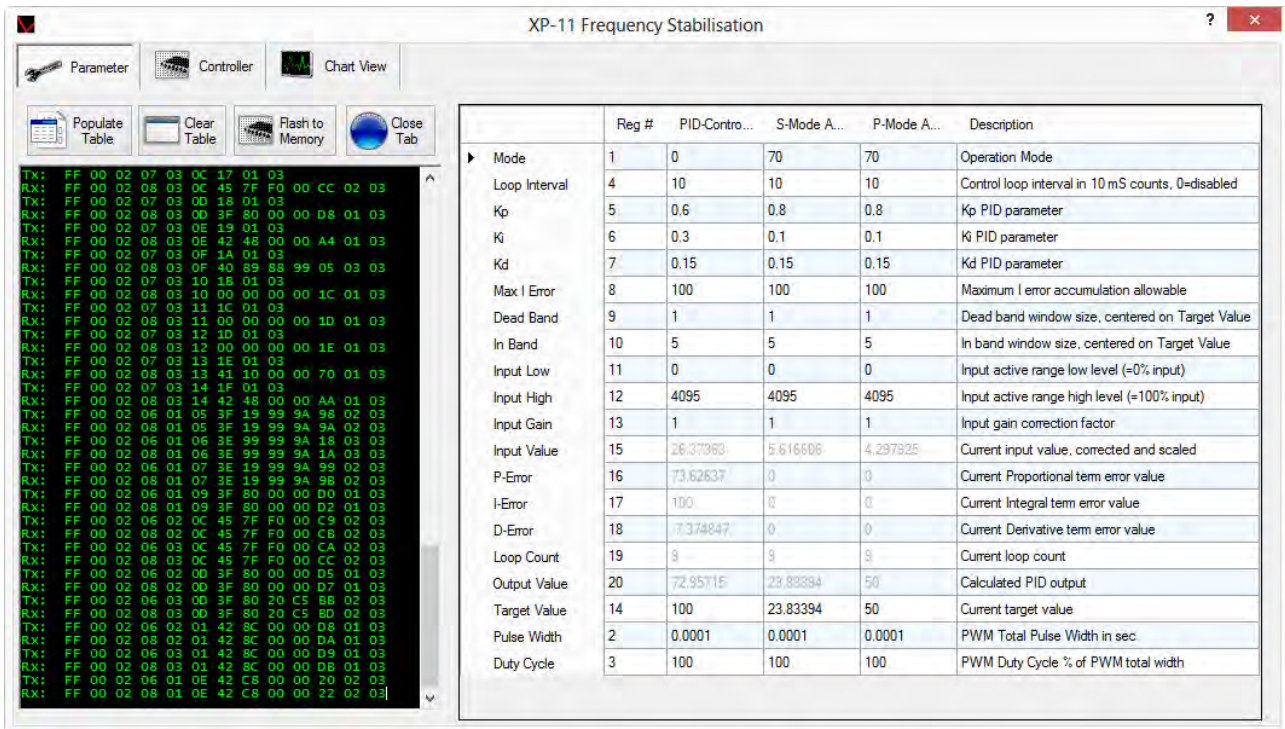
Fig. 38: Parameter expert view

In the parameter expert view the parameter as well as the communication protocol can be viewed and modified. This page is basically intended for trouble shooting.
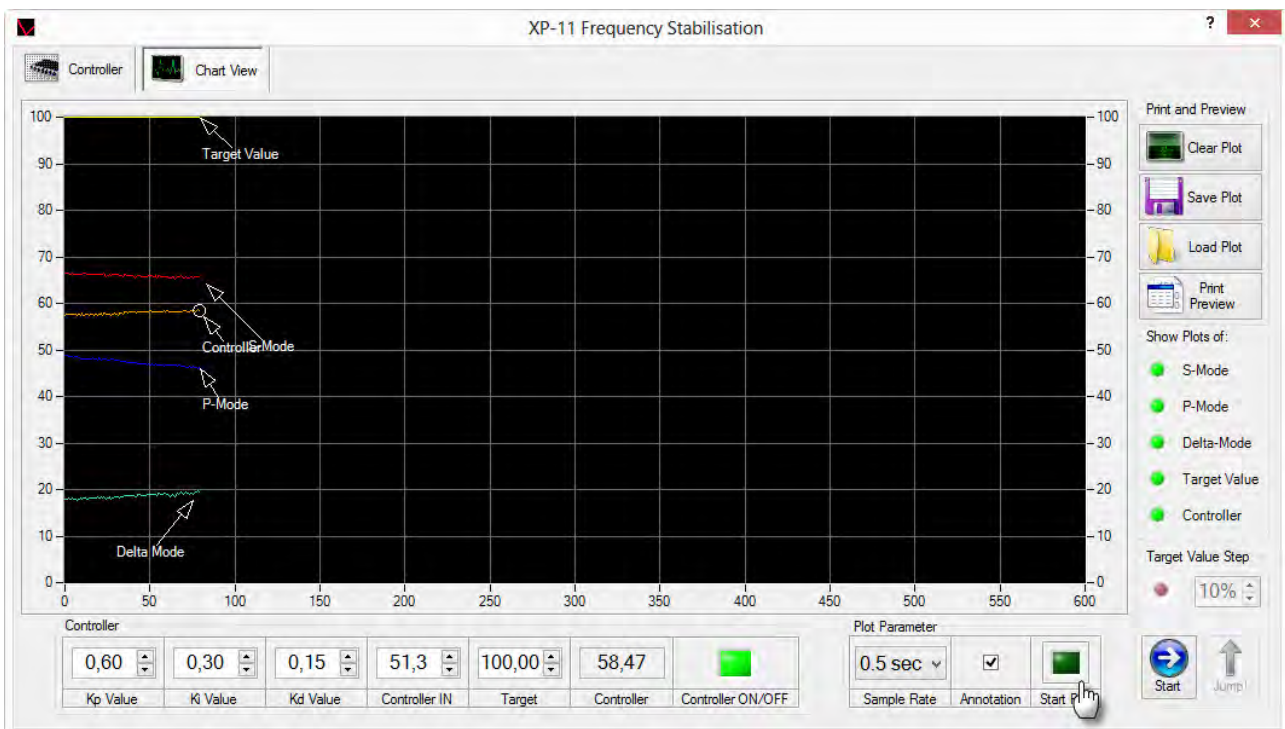

Fig. 39: Plot chart view

The plot chart view serves two purposes. It shows the time dependant plot with selected parameters like S-Mode, P-mode, Delta Mode (the difference of both modes which also is the controller input), the target value and the controller output. Within this view the controller parameter can be changed and its effect on the laser observed.

Secondly this view can be used to study fundamental controller properties. Here only the Delta mode (controller in), target value and controller output are displayed as chart strip. The target value can be set to a specific step value. By clicking on the "Jump" button send this information to the controller and the reaction of the controller is monitored and recorded.
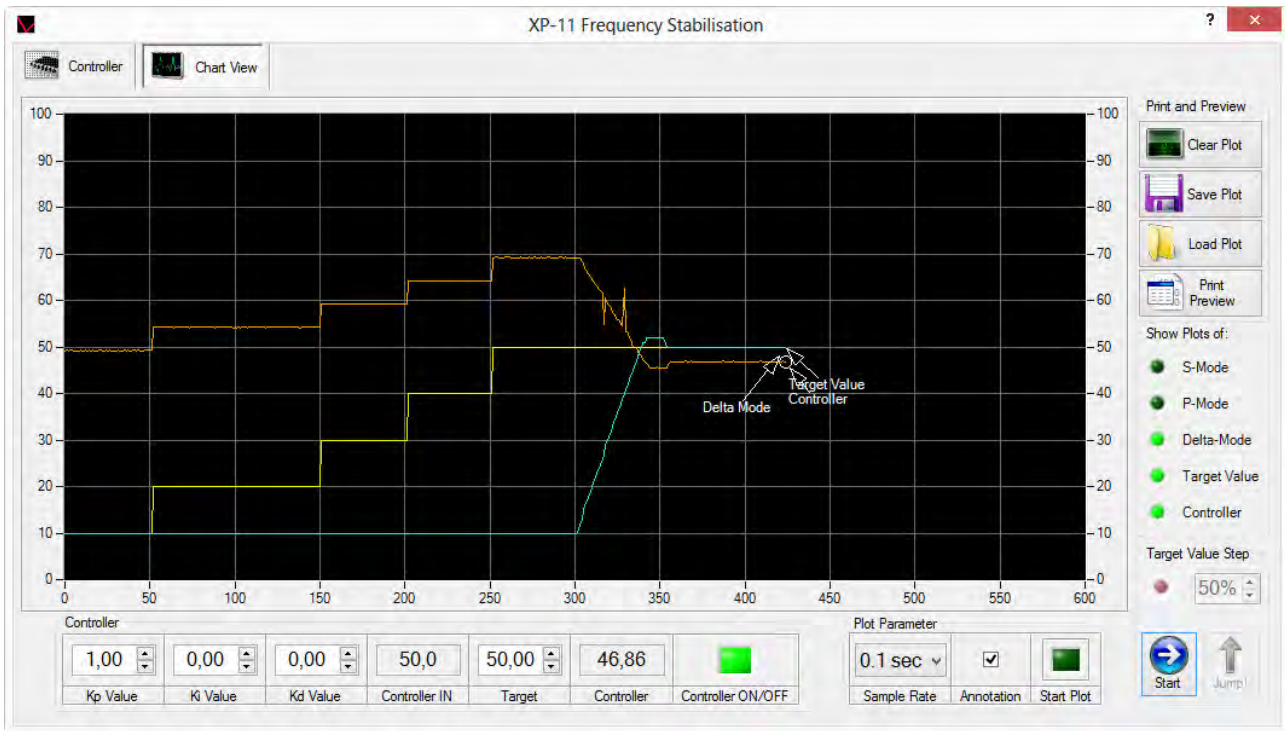
Fig. 40: Pure P controller

In the example of Fig. 40 the parameter has been chosen in such a way that the controller is a pure "P-controller". A jump of the target value leads to a proportional jump of the controller output.
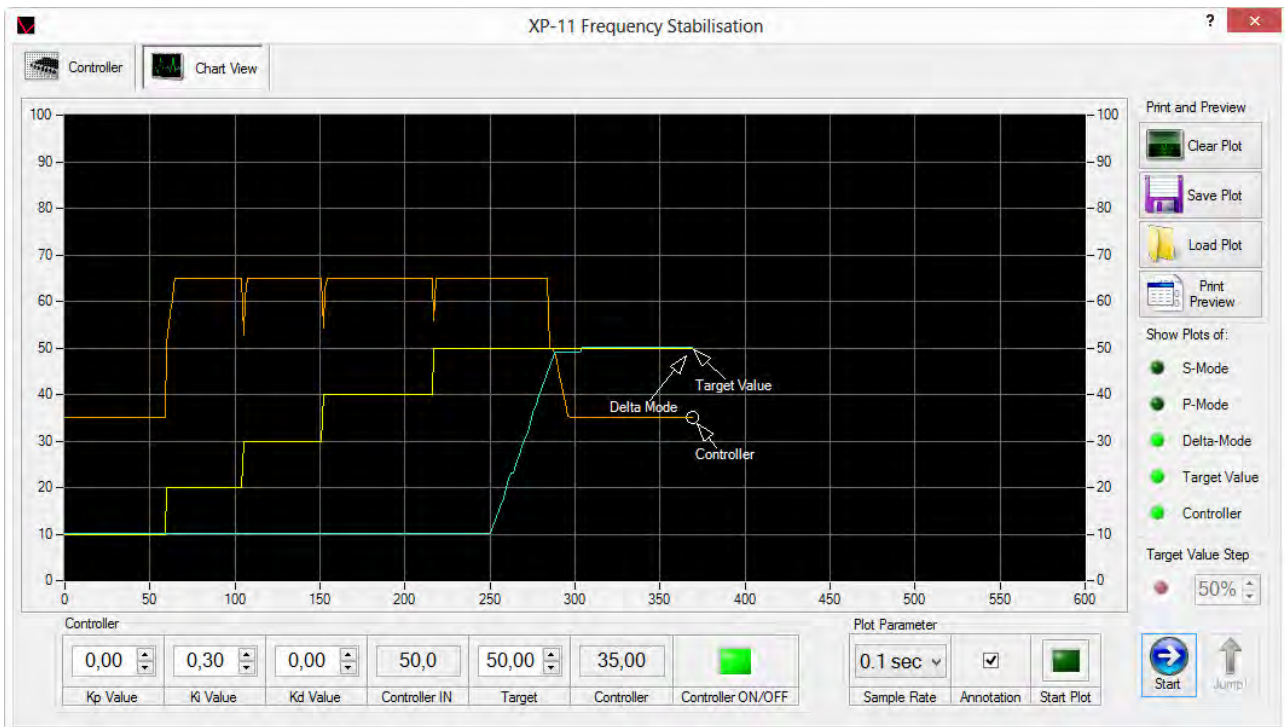
Fig. 41: Pure I controller

The example of the Fig. 41 shows a pure I controller. After the jump of the target value the controller output goes to its upper limit. Any additional jump in the target value leaves the controller in its limit value (the down peaks of the control signal are caused by the data transfer to the controller).
As soon as the controller in signal (Delta Mode) is changing the controller reacts accordingly.
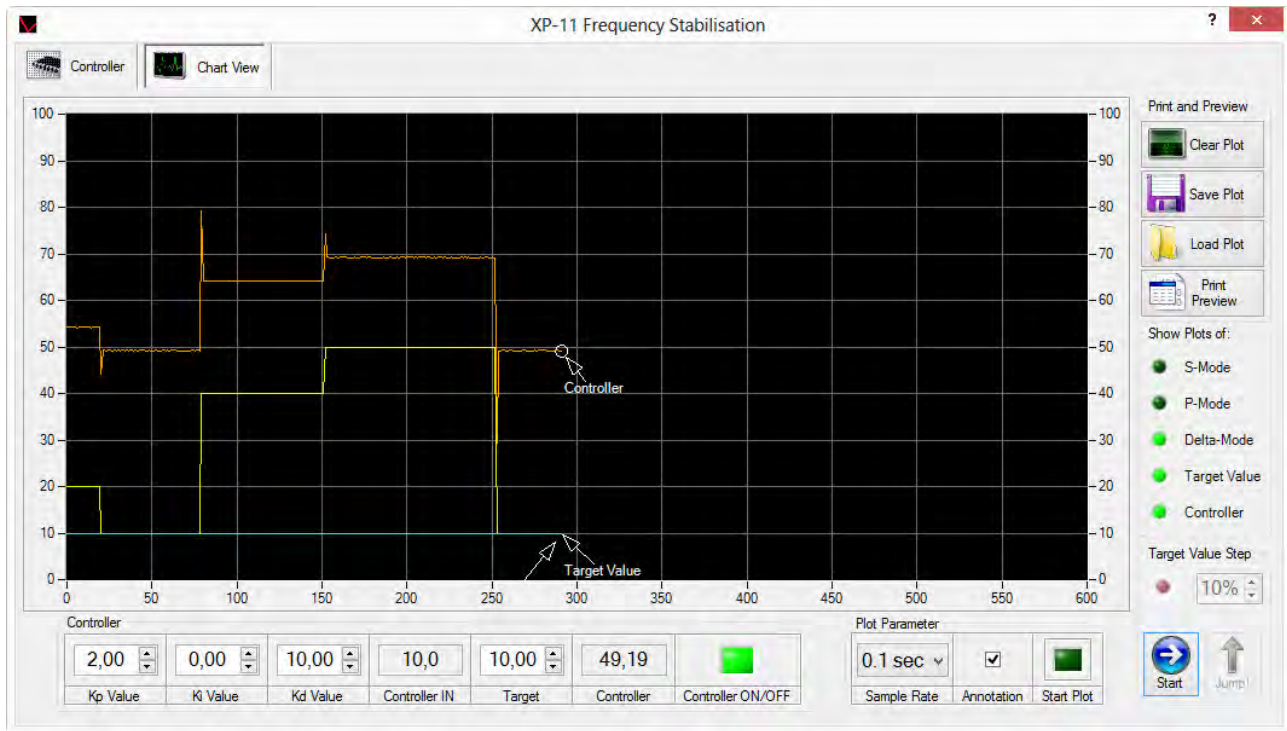
Fig. 42: PD controller

By changing the parameters to a PD controller, a jump of the target value provides an extra peak on top of the P-signal. This simple example of the controller simulation is useful to understand the basic principle of the controller technology and will be applied within the next experiments.
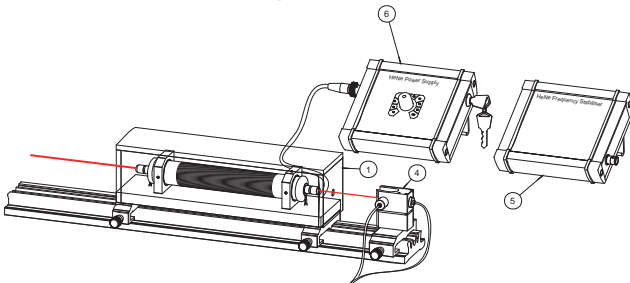
6.0 Experiments

6.1 Free running laser

Fig. 43: Setup for the mode detection and frequency stabilisation

The HeNe laser tube is connected to the high voltage supply (6) and the operation current set to 5.5 mA. The heater coil cable is connected via its 4 pin round connector to the control unit (5). Both photodetector of the mode splitting unit (4) are connected via their 3.5 mm stereo jacks to the control unit (5). The software is started and connected to the controller. In the chart view we select the S-Mode and P-Mode to be displayed. By clicking the "Start Plot" button starts the plot. After switching on the HeNe laser we will observe a mode sweeping chart as shown in Fig. 44. The extreme values of amplitude of the signal is related to the sweep range according to the spectral mode difference of about 800 MHz. This serves later as scale for the achieved frequency stabilisation. After a while (almost 30 minutes) the period of the sweep signal is reducing since the laser reaches its thermal equilibrium (Fig. 45).
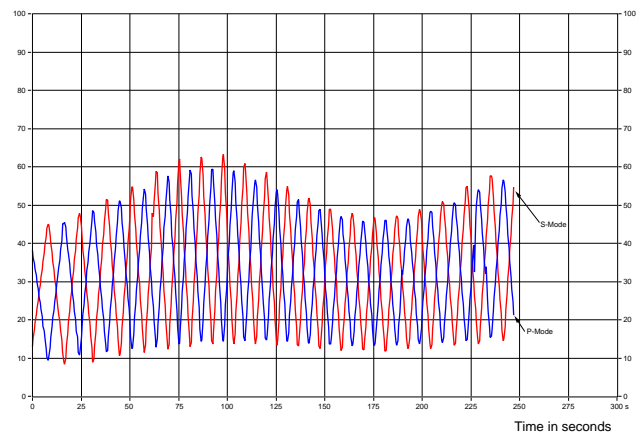

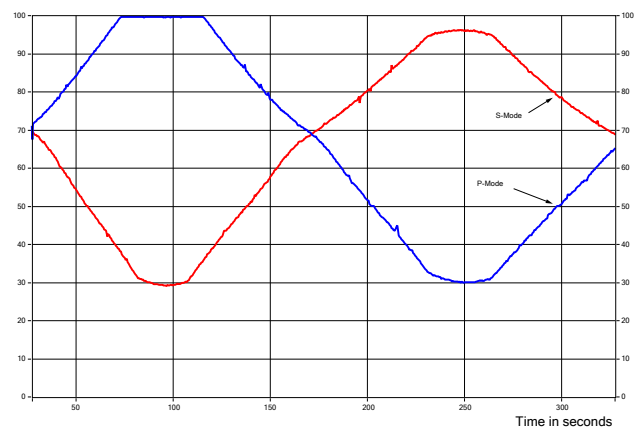**Fig. 44: Mode sweeping signal**

Fig. 45: Mode sweep close to the thermal equilibrium of the HeNe laser.
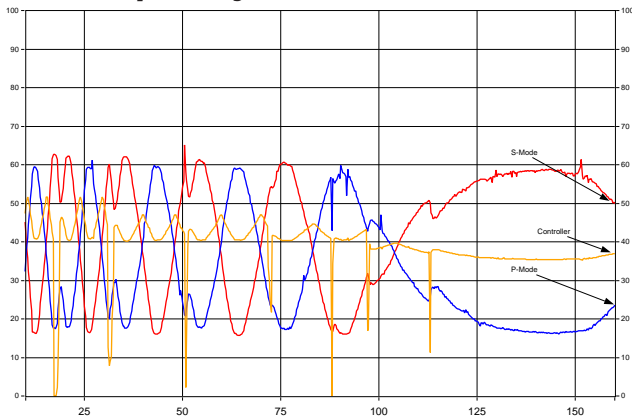
6.2 Frequency stabilisation

Fig. 46: Stabilisation attempt

After almost reaching the thermal equilibrium of the laser tube we can initiate the controller. For this purpose we switch on the controller by software. Furthermore the switch on top of the controller unit needs to be switched to "Frequency Stabilisation". in This mode the heater coil is connected to the controller and active. By modifying the controller parameter the mode signal is observed. Already the basic settings are suitable as shown in Fig. 46. The respective parameters are stored in the default.cfg file as well as in the memory of the controller. The default.cfg file can be loaded when clicking the "Load Parameter" button on the main screen.
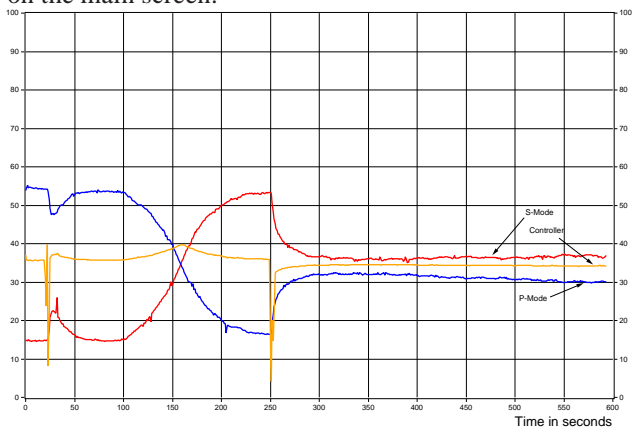

Fig. 47: Almost perfect controller settings

A further refinement of the parameter leads to an almost constant level of the mode signal. The achieved frequency variation Δν can be determined by

$$\Delta \nu = \frac{\Delta A}{A_{max} - A_{min}} \cdot 800\ MHz$$

Whereby ΔA is the amplitude variation taken from the plot and A_{max} and A_{min} the extreme values of the mode intensity variation. Finally a value of

$$\frac{\Delta \nu}{\nu} \leq 5 \cdot 10^{-8}$$

is a very good result. ν is the centre frequency of the HeNe laser and can be calculated by using

$$\nu = \frac{c}{\lambda}$$

The speed of light is c and λ is the wavelength of the HeNe laser 632.8 nm.
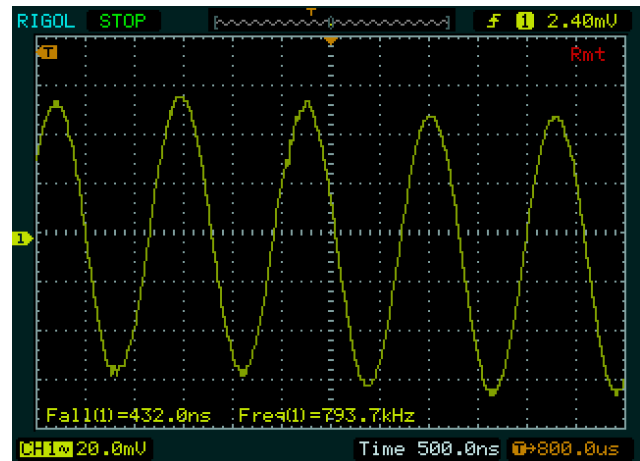
6.2.1 Zeeman Effect

Fig. 48: Zeeman beat frequency

The Zeeman beat frequency can only be observed when the magnet is placed into the marked area on top of the laser housing. The beat frequency occurs when the laser is tuned close to the centre frequency. This can be observed either in stabilised mode or by slowly mode sweeping. By means of an oscilloscope the signal of the photodetector (3) is displayed. The connection box (7) is switched to 10K resulting in a signal with an amplitude of almost 100 mV or more in AC mode of the oscilloscope. It is important to place the polariser (2) in front of the detector. The polariser must be set to 45° since we are observing the transversal Zeeman effect.
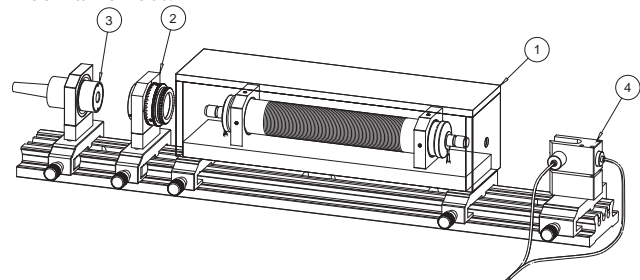

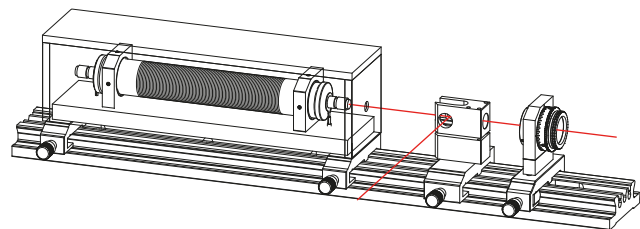Fig. 49: Setup with detector for beat frequency observation

Fig. 50: Calibration of the polariser

In case the polariser needs to be calibrated it is placed behind the mode separation unit where the photodiodes have been removed. The rotator of the polariser is set to 90°. The polariser itself can be unfastened and turned in such a way that no light transmits it. Fasten the polariser again, now it is calibrated.
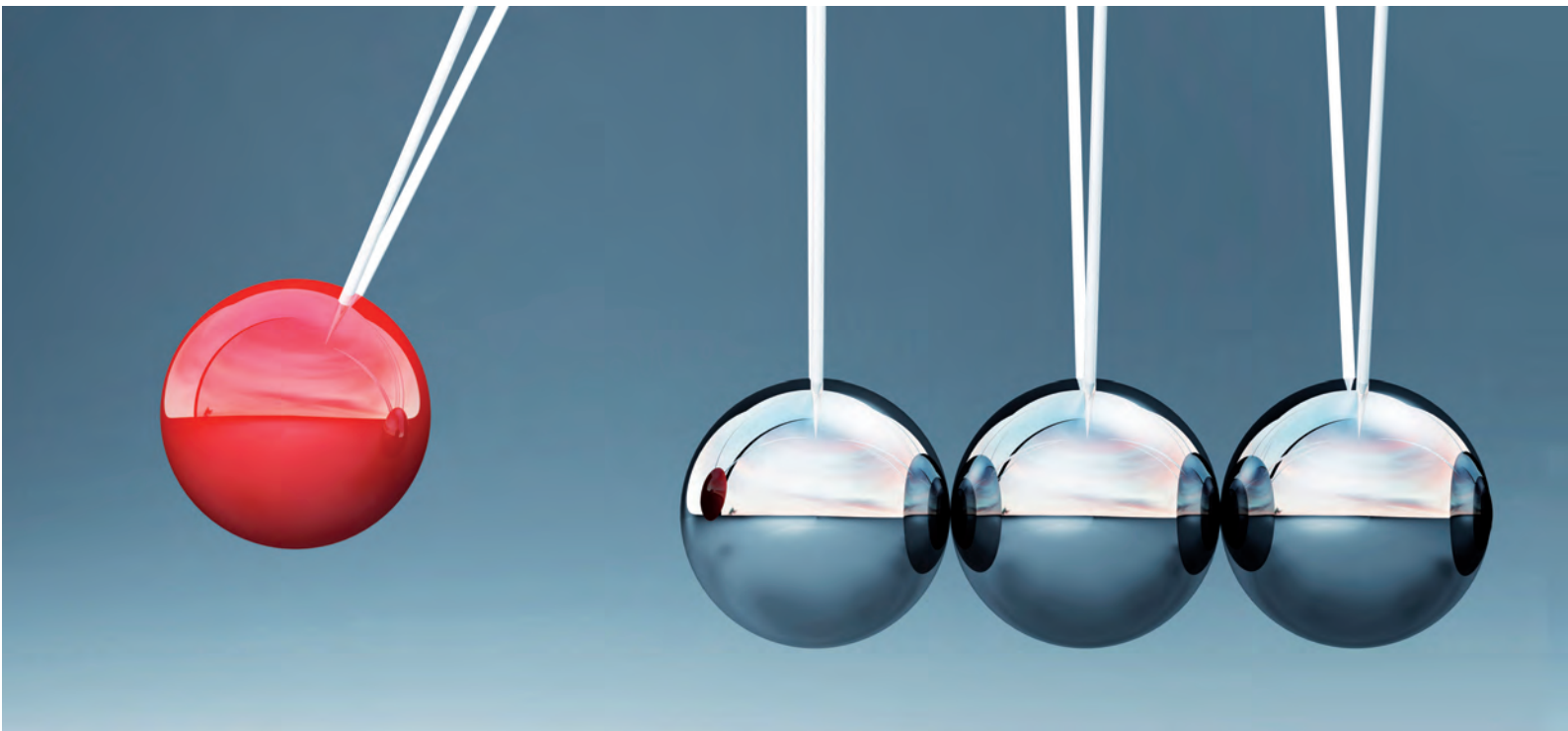
LD DIDACTIC

LD DIDACTIC distributes
its products and solutions
under the brand LEYBOLD

LEYBOLD®